7

Entrainment of material by debris flows

Oldrich Hungr, Scott McDougall, and Michael Bovis

7.1 INTRODUCTION

Debris-flow magnitude can be defined as the total volume of material moved to the deposition area during an event. It is an important quantity as it serves to scale the event and correlates with other parameters such as maximum discharge and runout distance (Chapters 13 and 17).

From descriptions in many other chapters of this book, it is clear that debris-flow magnitude is rarely determined by the volume of the initiating landslide. Often, the initiating slide is small and the bulk of the volume transported to the deposition area results from entrainment of material along the path. An excellent example is the 1990 Tsing Shan debris flow shown in Figure 7.1, the largest natural debris flow observed in Hong Kong (King, 1996). Here, a small slip of 400 m^3 enlarged to a final volume of 20,000 m^3 by entraining colluvium from the flow path. Figure 7.2 shows a reconstruction of the mass balance curve of this debris flow, based on data collected by King (1996).

Thus, it is the efficiency of the entrainment mechanism that primarily determines the total volume of a debris flow.

7.2 MECHANISMS OF MATERIAL ENTRAINMENT

Bedload in a stream channel lined with granular bed material can be transported by suspension, rolling, sliding, or saltation (e.g., Easterbrook, 1999). As shown in flume experiments, once the slope of the channel increases beyond approximately 10°, the bed itself may become unstable under the combination of gravity and drag forces imposed by the over-riding water flow (Bagnold, 1966). If the surface fluid is saturated debris instead of water, even greater drag forces result and the bed material can be massively mobilized and entrained into the flow.

M. Jakob and O. Hungr (eds), *Debris-flow Hazards and Related Phenomena*.

Figure 7.1. The Tsing Shan debris flow that started as a small debris slide of 400 m^3 and grew to a total magnitude of 20,000 m^3 through material entrainment.

Photo courtesy, J. King, Geotechnical Engineering Office, Hong Kong.

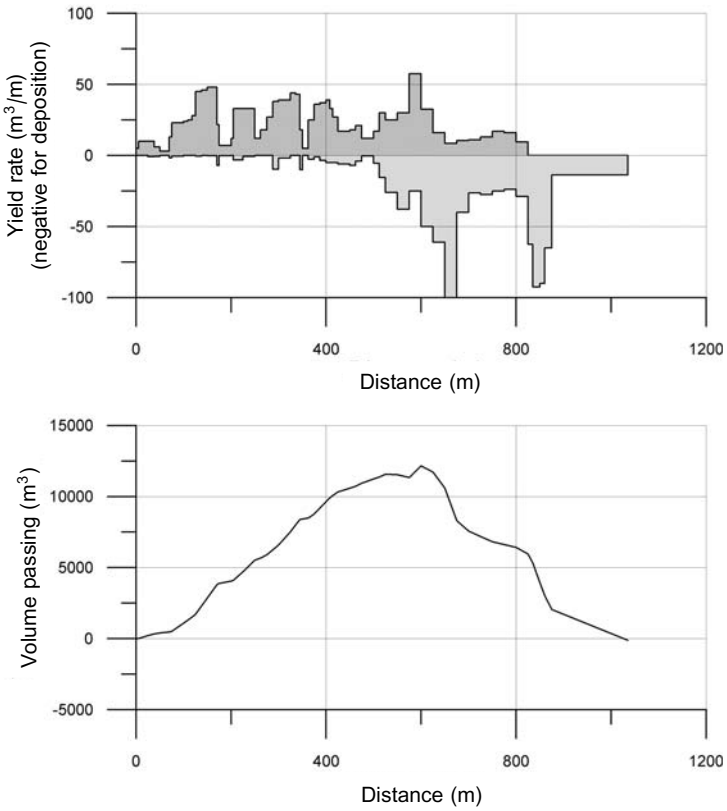

Figure 7.2. Tsing Shan debris flow. (a) Distribution of observed yield rate. (b) Approximate mass balance curve.

Based on data reported by King (1996).

The process of surge formation, resulting from longitudinal sorting and the emergence of boulder fronts (e.g. Iverson, 1997) or from the formation of turbulent fronts (e.g. Davies, 1986), magnifies the peak discharge of debris-flow surges (Hungr, 2000) and is thus likely responsible for an increase in drag forces and further enhancement of the entrainment intensity.

One of the mechanisms causing material entrainment in debris flows is bed destabilization and erosion. Destabilization of bed material is the result of drag forces acting at the base of the flow, but may be aided by strength loss due to rapid undrained loading (Hutchinson and Bhandari, 1971), impact loading, and liquefaction of the saturated channel fill (Sassa, 1985, see also Chapter 5). As shown schematically in Figure 7.3, bed destabilization during a debris flow may affect not only bedload, but any erodible bed substrate. This process of bed destabilization can be quantified to some degree as shown in the following section, although the necessary data regarding bed stratigraphy, bed material, substrate strength, and drainage characteristics is difficult to obtain. Knowledge of erosion

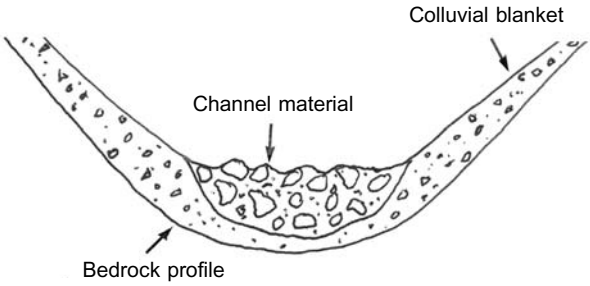

Figure 7.3. Schematic diagram of an eroded vertical cross section of a debris-flow channel.

depth is also useful for practical purposes, such as the protection of pipelines crossing a debris-flow channel (Jakob et al., 2004b).

The second important mechanism of material entrainment results from instability of stream banks undercut by bed erosion, as also shown in Figure 7.3. It is important to consider that steep stream and gully channels are often being actively incised. Thus, their banks may exist in a state of marginal equilibrium that is easily disturbed by lowering of the bed, such as often occurs during passage of a debris-flow surge. The bank may respond immediately and release a shallow landslide directly into the body of the surge, or may release with a delay, to provide material available for incorporation into the next surge. Thus, some debris may form transient deposits in the channel, only to be re-mobilized later during the same event, or in a later event. Eyewitness reports mention debris from bank slides that briefly dam the channel and are then rapidly eroded by overtopping water or debris flow, and are readily liquefied by mixing with stream water (Johnson, 1970). Such processes are complex and defy mechanistic quantification, since the required data on side slope stability, including strength provided by vegetation, and the temporal relationships between surging flow discharge, bed erosion, bank slope failure, and mixing of water and debris, cannot normally be obtained. A photo of a channel combining highly erodible bed and banks is shown in Figure 7.4.

7.3 THEORETICAL APPROACH: BED STABILITY

The process of bed destabilization during a debris flow can be represented by a simple extension of the infinite slope stability theory (e.g. Morgenstern and Sangrey, 1978). However, much depends on the assumptions made concerning pore-water pressure in the bed materials. In the first attempt at deriving a formula for the depth of bed instability, Takahashi (1978, 1991) assumed slope-parallel seepage in a saturated bed. In the following derivation we use different symbols than Takahashi (1978), but the same physical concept.

The problem configuration is shown schematically in Figure 7.5. A sheet of debris, of thickness z_d, flows over a bed of cohesionless material inclined at an angle β. As a result of the added tractive force of the debris, the bed becomes

Figure 7.4. An eroded debris flow channel in the Columbia Mountains, British Columbia. Material was derived both from vertical erosion of the bed and from instability of the banks.

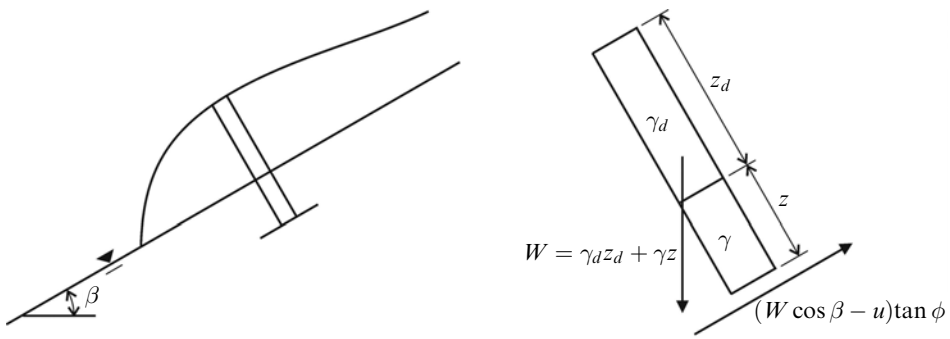

Figure 7.5. (a) Schematic representation of a saturated bed over-ridden by a debris flow, showing a slope-normal column of unit length and width. (b) Forces acting on the column in (a) include the weight of the column and the shear resistance at its base. Loading due to the over-riding flow destabilizes the bed to depth z. See text for details.

unstable to an unknown depth z below the original bed surface. As is standard in the infinite slope approach, only the stability of a typical column of a unit length in the downslope direction is considered (the width perpendicular to the flow is unity).

Based on the diagram of the column shown in Figure 7.5, its weight equals:

$$W = \gamma_d z_d + \gamma z \tag{7.1}$$

where γ is the saturated unit weight of the bed material (typically 20–23 $\mathrm{kN/m^3}$) and γ_d is the bulk unit weight of the debris (18–20 $\mathrm{kN/m^3}$).

From Figure 7.5, the normal total stress at the column base equals:

$$\sigma = W \cos\beta \tag{7.2}$$

The shear stress equals:

$$\tau = W \sin\beta \tag{7.3}$$

Takahashi (1978) assumed slope-parallel seepage and uniform flow, combined with instant drainage, so that the pore fluid is hydrostatically pressurized and flowing in a steady-state regime, with no excess pore pressure. Such assumptions may not be justified, as discussed below. However, to continue the analysis, with these assumptions the pore pressure at the base of the column is:

$$u = \gamma_w (z_d + z) \cos\beta \tag{7.4}$$

where γ_w is the unit weight of water and $(z_d + z)\cos\beta$ is the elevation difference measured along an equipotential line.

The shear strength of the bed material is given by the cohesionless Mohr–Coulomb shear strength equation, in which ϕ is the friction angle:

$$S = (\sigma - u) \tan\phi \tag{7.5}$$

At the point of shear failure $S = \tau$. Hence, from (7.2), (7.3), and (7.5):

$$(W \cos\beta - u) \tan\phi = W \sin\beta \tag{7.6}$$

Substituting further using (1) and (4) and solving for z:

$$z = z_d \left[\frac{\dfrac{\gamma_d}{\gamma}\left(1 - \dfrac{\tan\beta}{\tan\varphi}\right) - \dfrac{\gamma_w}{\gamma}}{\dfrac{\gamma_w}{\gamma} - \left(1 - \dfrac{\tan\beta}{\tan\varphi}\right)} \right] \tag{7.7}$$

This equation is equivalent to Takahashi's (1978, Equation 22). Its results are represented by the dashed lines in Figure 7.6. The saturated unit weight of the bed material was chosen as 20 $\mathrm{kN/m^3}$ (i.e., about twice the unit weight of water). Therefore, by application of the simple infinite slope stability equation, the ratio $\tan\beta/\tan\phi$ must be less than about 0.5, or the bed itself would be inherently unstable. The diagram shows that a certain amount of entrainment is possible for any value of γ_d less than $\gamma_w/(1 - \tan\beta/\tan\phi)$, with more dilute flows causing instability to greater depths. For fully developed debris surges, whose bulk density approximates the density of the bed material (i.e., $\gamma_d/\gamma = 1$), no entrainment will be predicted with these assumptions, except if the bed itself is inherently unstable.

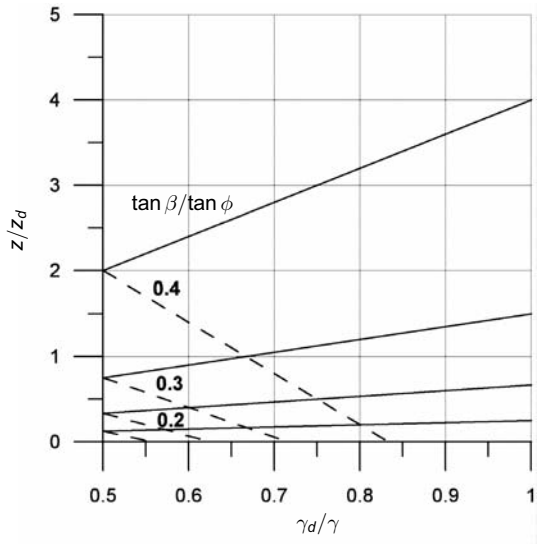

Figure 7.6. Erosion depths predicted by solution of (7.7) (dashed lines) and (7.9) (solid lines).

Debris-flow surges travel many metres per second and, even with a relatively coarse and pervious bed material, it is unlikely that a steady seepage condition can be achieved in the short time while a surge peak is passing. A more realistic assumption is that the full bulk weight of the debris flow $\gamma_d z_d$ will be transferred to pore-water by undrained loading, generating geostatic pressure within the bed materials. Thus, instead of (7.4) we have:

$$u = (z_d \gamma_d + z\gamma_w)\cos\beta \tag{7.8}$$

Following the same steps that have led to (7.7) we obtain:

$$z = z_d \left[\frac{-\dfrac{\gamma_d}{\gamma}\dfrac{\tan\beta}{\tan\varphi}}{\dfrac{\gamma_w}{\gamma} - \left(1 - \dfrac{\tan\beta}{\tan\varphi}\right)} \right] \tag{7.9}$$

This equation is plotted using the full lines in Figure 7.6. Here, a very different trend is observed. The unstable depth *increases* with the bulk density of the debris flow and entrainment is predicted for all values of γ_d and β, as long as the bed is not horizontal. The actual value of the unstable depth may lie somewhere between the two extremes depicted in Figure 7.6 although it is likely closer to the undrained condition (full lines) than those for the drained condition.

While these results are conceptually interesting, they are of little value for practical application. One reason is that little is known about the shear strength of materials comprising the bed of a debris-flow stream and its variation with depth. Often, there will be a layer of cohesionless, coarse material, underlain by a substrate possessing either true or apparent cohesion, such as glacial till or residual soil.

Pore-pressures are also unlikely to be easily predictable, due to possible discharge gradients at the base of a steep-sided path segment or excess gradients generated by rapid loading and vibration due to the debris flow. Three-dimensional effects (i.e., the strength of lateral surfaces at the channel edge), are also likely to be important. Although the equations may help predict when erosion will begin to occur, the rate at which material is entrained into the flow requires further analysis and further difficult assumptions. Thus, the above equations can be regarded merely as conceptual guidelines. As argued in the preceding section, the process of entrainment involving bank instability is even less amenable to mechanistic analysis. Consequently, the remainder of this chapter concentrates on empirical approaches to the problem.

7.4 THE YIELD RATE AND EROSION DEPTH CONCEPTS

Several early empirical algorithms for prediction of debris-flow magnitude were reviewed by VanDine (1985). Some of these methods attempt to correlate magnitude with the drainage area, but the results tend to be widely scattered (see Chapter 17). Other methods concentrate on erosion of material along the length of channels. The first such published attempt was Ikeya (1981), who suggested that potential magnitude can be calculated as a product of the channel length L, mean width B, and mean erosion depth D. He used empirical relationships involving drainage area for L and B and estimated D as ranging between 0.5 and 3.2 m.

A more direct method was developed by Thurber Consultants (1983) and Hungr et al. (1984), based on the concept of yield rate Y_i. The yield rate is defined as the volume eroded per metre of channel length (Hungr et al., 1984). With reference to Figure 7.3, it is the area of the vertical cross section of the eroded space, multiplied by the cosine of the channel slope angle β to convert vertical depth to thickness. To apply the concept, the channel system of a debris-flow watershed is divided into channel reaches considered to be approximately constant in terms of the parameters critical for material entrainment, as listed in Table 7.1.

Once the applicable yield rates are estimated, the debris-flow magnitude (volume) V(in m^3) can be estimated by the formula:

$$V = V_{initial} + \sum V_{point} + \sum_{i=1}^{n} Y_i L_i \tag{7.10}$$

Here, $V_{initial}$ represents the volume of the initiating landslide, V_{point} is the volume of any "point sources" (i.e., tributary landslides that may be destabilized by a passing debris flow and add volume to the flow), and L_i and Y_i are the length and yield rate of n channel reaches as defined above.

While the concept represented by (7.10) is simple, several problems remain. First is the optimal number of tributaries to the main debris-flow channel to include in the summation. Some debris flows affect only one branch at a time. Other events, especially those triggered by a major regional storm, may mobilize nearly every

Table 7.1. Parameters relevant to the yield rate Y_i

Slope angle
Existing channel width and depth
Bed material
Bank slope angle
Bank slope height
Bank slope material
Bank slope stability rating
Tributary drainage area or discharge

tributary of the drainage network, right down to zero-order colluvial hollows (Figure 7.7). To the authors' knowledge, no research clarifies this issue, and a judgmental decision needs to be made based on local experience. Knowledge of the time elapsed since the last debris flow may provide some guidance, since this controls the amount of debris replenishment in formerly scoured channel segments. This issue is further discussed in Chapter 17.

In exceptional cases of catastrophic rainstorms, the extent of instability of steep slopes in the headwaters may be so large as to make the yield rate approach impractical. For example, the December 1999 storm in the Vargas State, Venezuela, caused the failure of up to 30% of the steep slopes in certain basins (Lopez et al., 2003; see Chapter 20). The magnitude of debris produced by such events may best be estimated by multiplying the predicted area of landslide scars by the average erosion depth.

The second problematic issue is determination of the downstream limits of debris-flow erosion. It is well known that debris-flow surges erode material on steep slopes, but deposit material on slopes flatter than a certain limit. Several suggestions for setting the deposition slope can be found in the literature:

1. Ikeya (1981), followed by Okubo and Mizuyama (1981), suggested a slope of 10°.
2. Hungr et al. (1984), referring to relatively coarse-grained non-volcanic debris flows from Southern British Columbia, Canada, suggested a deposition slope of 8–12° for "confined" channels and 10–14° for "open" channels, the former being characterized by a maximum flow depth/width ratio of over 1 : 5.
3. Small debris flows and debris avalanches in Hong Kong often deposit on slopes exceeding 30–40° (Wong et al., 1997).
4. Referring to debris flows from the Pacific North-west, USA, Benda and Cundy (1990) placed the downstream end of erosion at a 10° slope. Deposition is said to begin at a slope of 3.5°, or earlier if a sharp change of flow direction occurs at a stream junction.
5. Fannin and Wise (2001), using data from coastal and insular British Columbia, found both deposition and entrainment occurring on slopes of 10–22° in confined reaches and 19–24° in unconfined ones (e.g., open slopes, gully sidewalls or headwalls).

Figure 7.7. A debris flow channel with multiple branches in Banff National Park, Canada. Photo D. Ayotte.

6. Jordan (1994) made a comparison between coarse-grained debris flows derived from igneous rocks of the Coast Plutonic Complex, southern British Columbia, Canada and fine-textured volcanogenic debris flows from the same region. The average slope angles of the deposits ranged between 7 and 15° for the former and 0.5 to 5° for the latter, showing a strong inverse relationship to volume (ranging up to $10^7\,m^3$ for the largest lahars).
7. Large debris flows from metamorphic rock sources, triggered during the 1999 Vargas State disaster in Venezuela, eroded fan and floodplain deposits and carried large boulders to slopes as low as 2° without substantial confinement (Lopez et al., 2003, see also Chapter 20).
8. Large, eruption-triggered debris flows on volcanoes may erode substantially on slopes as flat as 1° (Pierson, 1995, see also Chapters 10 and 27).

This collection of deposition criteria confirms the disquieting fact that no general guidelines for the determination of the deposition angle exist. Furthermore, experience shows that smaller debris flow and debris avalanche events can deposit on considerably steeper angles than larger events on the same path. Mean water content of individual surges also seems to play an important role as does the composition and particle size of the surge front. Thus, the downstream limit of erosion may vary from one event to another, or even between individual surges.

Research is needed to establish two criteria: the slope where substantial erosion ends (''limit of erosion slope'') β_e, and the slope where deposition begins (''slope of deposition'') β_d (neither may be a unique value for a given path). The factors likely to influence both limits are probably those listed in Table 7.1. Both angles will probably be strongly affected by the average solids concentration of a debris-flow surge. Flows with lower solids concentrations by volume should be more erosive and also should have the lowest deposition angles. The implication of this is that relatively steep fan accumulations of material laid down by one flow may subsequently be eroded and remobilized by later flows having lower solids concentrations. This type of behavior is observable on many debris fans, where complex patterns of filling and cutting tend to be the rule rather than the exception.

The third problem is the estimation of the yield rate itself. Some channels and gullies are formed in substrate of low erodibility (e.g., bedrock or dense or very coarse granular soil or stiff cohesive soil). Bedload material and colluvial wedges at the base of stable banks are ephemeral in such channels and likely to be eroded by a climax debris-flow surge. An example of such a ''firm-base channel'', formed in igneous bedrock, is shown in Figure 7.8. The corresponding term in sediment hydraulics is a ''supply-limited'' channel (cf. Bovis and Jakob, 1999; Jakob et al., 2004). It is possible to estimate the amount of debris available in firm-base channels by a direct visual inspection (Thurber, 1983; Hungr et al., 1984; VanDine, 1985).

Estimation of the yield rate is more difficult and subjective for ''erodible-base channels'', where no shallow, firm substrate exists and the entrainment process is transport-limited. As stated earlier, a theoretical means of estimating erosion depths in such cases is not practically useful, and recourse must be taken to subjective judgment, or empirical relations as discussed later in this chapter.

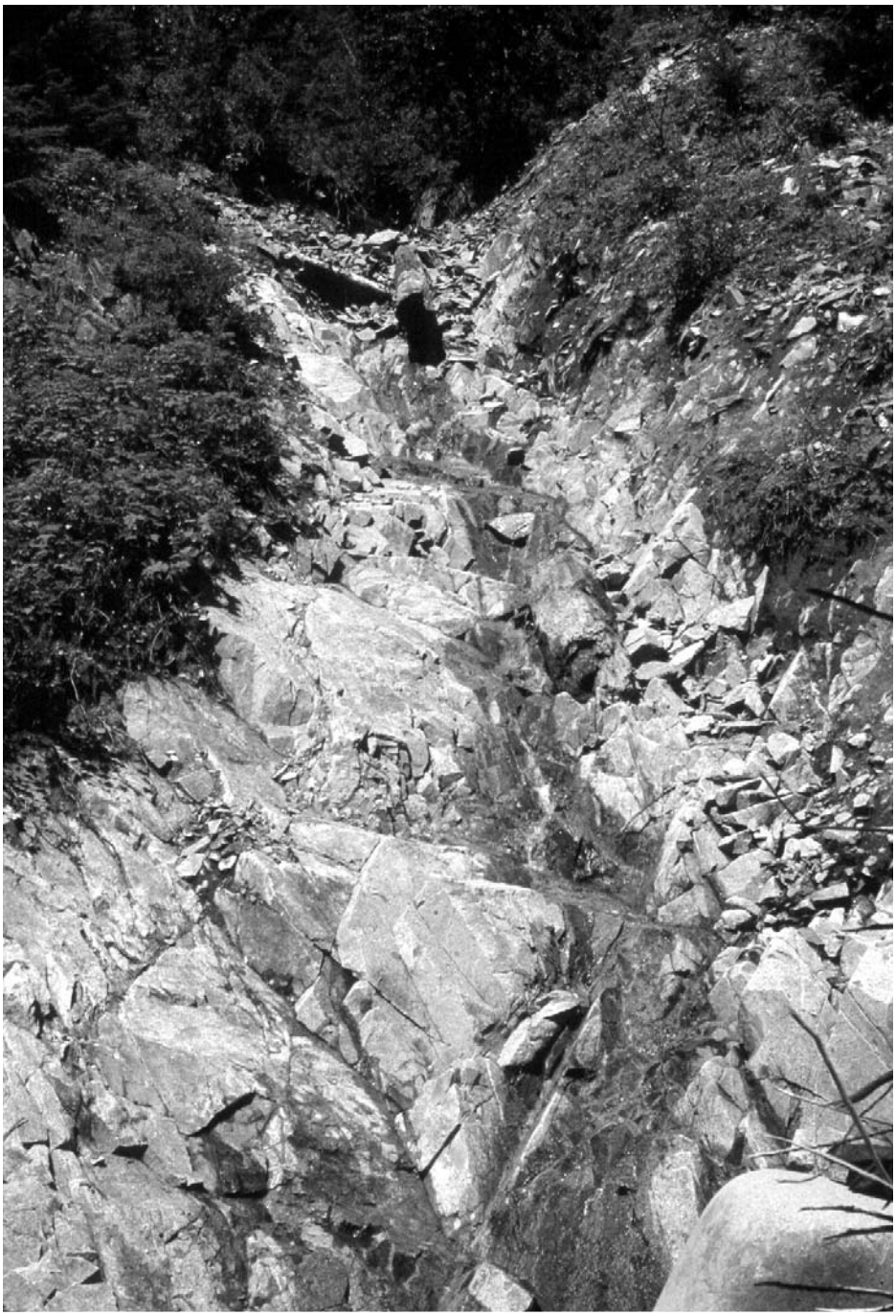

Figure 7.8. A photo of a firm-base channel, with a substrate of igneous bedrock, near Chilliwack, British Columbia, Canada.

The yield rate approach is difficult to use for unchannellized debris avalanches, where the yield rate depends strongly on the width of the path. In this case, the ''erosion depth'' parameter is a more suitable index for estimating volumes, provided that the width of the path is known. The relation between yield rate (Y_i, in m^3/m), erosion depth (D_i in m), and path width (B_i in m) is:

$$Y_i = B_i \times D_i \tag{7.11}$$

Here the index i represents a particular reach of a path. The erosion depth in open-slope debris slides depends primarily on the depth of any loose layer such as a colluvial veneer, an organic rich soil horizon, or a loosened surficial layer. In some cases, it can be estimated directly from field observation or by subsurface investigations such as test pits or geophysical surveys.

Path width is another parameter that is difficult to estimate, except in the case of firm-based channels. Width estimation is particularly difficult on open slopes, where debris avalanche scars are often observed to widen with distance downslope (Figure 7.9). Guadagno et al. (2003) suggested empirical means to estimate the angle of spreading of debris avalanche scars in the Campania Region, Italy (Chapter 19).

A collection of reported values of erosion depth and yield rate from several parts of the world is shown in Table 7.2, which shows that depth ranges up to about 6 m and yield rate up to about $30\,m^3/m$, although much larger values probably occur in

Figure 7.9. Two debris avalanches widening with distance downslope. (Quindici, Campania Region, southern Italy.)

Table 7.2. A collection of debris flow entrainment rates and erosion depths reported in the literature.

Reference	Location	No. events	Confinement	Erosion depth (m)	Yield rate (m^3/m)
Hungr et al. (1984)	B.C. Coast, Canada	5	C	–	6–18
Jakob et al. (1997)	B.C. Coast, Canada	2	C	–	(23)
Campbell and Church (2003)	B.C. Coast, Canada	37	C	0.5–1	–
Fannin and Rollerson (1993)	Queen Charlotte Island, Canada	253	C	–	(12.6)
		196	U		(24)
Jakob et al. (2000)	B.C. Interior, Canada	1	C	0.5–1.5	(28)
Cenderelli and Kite (1998)	The Appalachians, USA	4	U	0–2.5	0–42 (4.2)
Springer et al. (2001)	The Appalachians, USA	2	C	–	2–18
Agostino and Marchi (2003)	Southern Alps, Italy	1	C	0.1–6 (1.0)	–
Revellino et al. (2003)	Campania, Italy	17	C, U	(1.5)	–
Li and Yuan (1983)	South-west China	1	C	5–8	–
Franks (1999)	Hong Kong	40	C	–	0.2–5 (3.6)
King (1996)	Hong Kong	1	U	0–3	0–50
Okuda et al. (1980)	The Alps, Japan	1	C	0–5	–
Rickenmann et al. (2003)	Kazakhstan	1	C	–	8–300

C = mainly confined events (debris flows), U = mainly unconfined events (debris avalanches).
Values in brackets are averages.

catastrophic events (see Chapter 27). The largest values in the table relate to reaches with large bank failures (Rickenmann et al., 2003).

7.5 CONSIDERATION OF FREQUENCY

The above discussion has attempted to present a deterministic picture. However, in reality, all of the parameters contributing to (7.10), including length of the eroded channels, location of the end of erosion, and the yield rate or erosion depth, are stochastic in nature. Thus, we are faced not only with the need to estimate the mean values of these parameters, but also their variance. Some attempts have been made to take a stochastic approach to this problem as discussed below. However, in many practical applications, the analysis focuses on determination of a flow "design magnitude" for a particular channel, which could be defined as the magnitude of an event whose probability of occurrence approximates the inverse of the expected lifetime of a given structure – such as a debris-flow basin – reduced by a suitable factor of safety (Thurber, 1983). The empirical calibration process could then be based on previous events with similar return periods.

Event return periods may be estimated more reliably for firm-base channels. If the path is underlain by a firm base, a debris flow may remove most of the loose material accumulated on it. Following the debris flow, there is no unconsolidated material available and a second event cannot happen. Gradually, more debris accumulates by erosion and mass movement from the hillsides adjacent to the path and by bedload deposition, thus "priming" the channel for another event (Bovis and Dagg, 1988). Bovis and Jakob (1999), found that debris flows can reoccur in some gullies of coastal British Columbia at intervals as short as a few decades. Benda and Dunne (1997), on the other hand, estimated that recharge times for gullies in the US Pacific North-west may be as high as several thousand years. Thus, no simple rule can be given at present.

7.6 EXAMPLES OF EMPIRICAL CALIBRATION OF THE YIELD RATE CONCEPT

The use of the yield rate concept was extended to the simulation of the deposition behavior of debris flows and avalanches on Oahu Island, Hawaii by Cannon (1993). She assumed that each event begins as a discrete debris slide, the volume of which can be estimated beforehand by independent means. A constant "lag rate" is then assumed, being the equivalent of the yield rate, but negative in this case, since material is gradually discarded along the path in levees and sheets. The runout distance is determined by dividing the slide volume by the lag rate. Using multiple regression analysis, Cannon (1993) found an empirical relation connecting lag rate with slope and width of the path (lateral confinement). Cannon's approach is difficult to apply in many cases of debris flows and avalanches, in which the volume of the initiating slide tends to be only a small fraction of the total volume mobilized along

the path, and where runout distance is usually significantly controlled by lateral spreading.

Fannin and Wise (2001), using data from the Queen Charlotte Islands of British Columbia, combined both the yield rate and lag rate approaches. Erosion tends to be dominant in the steeper reaches of the path, causing down-channel increases in flow volume. As slope angle decreases, deposition begins and volume is discarded according to a negative lag rate. Runout is predicted when the deposited volume equals the total entrained (i.e., a volume balance is established).

Fannin and Wise's (2001) approach was different from the concepts discussed here, in that neither yield rate nor erosion depth were used explicitly. Instead, regression equations were developed for incremental volumes of erosion and deposition per reach. Separate correlation equations were developed for reaches dominated by erosion and deposition and for transitional reaches. The primary predictor variables in the regressions included reach length and path width. Their correlation coefficients were close to 1, suggesting that these two quantities serve primarily as scaling factors. Thus, the use of incremental volumes instead of yield rates does not seem to be advantageous. Weaker, highly scattered correlations were also found for some path types with slope angle, lateral confinement, cumulative passing volume, and angular changes in flow direction.

The yield rate method was also examined by Lau and Woods (1997) for debris flows and avalanches in Hong Kong. They developed stepwise regression equations for the average yield rate of a channel, based on material type (colluvium, residual soil), slope morphology (planar, concave, convex), vegetation type, slope angle, and radius of channel cross section. However, they concluded that the correlations were very weak, and that the resulting model was no more consistent than the routine empirical runout estimation method based on the travel angle.

7.7 THE BRITISH COLUMBIA DEBRIS-FLOW DATABASE

T. Rollerson and T. Millard, scientists employed by the MacMillan Bloedel Company in British Columbia, investigated 449 debris flow and debris avalanche events from the Queen Charlotte Islands, British Columbia. The region is a heavily dissected plateau with a relief of sea level to approximately 700 m, composed of metamorphosed volcanics and sediments mantled by Pleistocene glacial soils and colluvium (Fannin and Rollerson, 1993). It has a cool, perhumid maritime climate, with an annual precipitation of 1,000–4,000 mm.

The full length of each landslide was traversed on the ground and estimates were made of material eroded and deposited in reaches judged to be homogeneous. An additional 39 events were studied subsequently on the south-western British Columbia coast by Wise (1997) and Yonin and Hungr (unpublished). After eliminating internally inconsistent and incomplete records, a database of 174 debris flow and debris avalanche events, comprising 1,073 channel reaches, was compiled. Unfortunately, the database does not contain any descriptive information on the reaches,

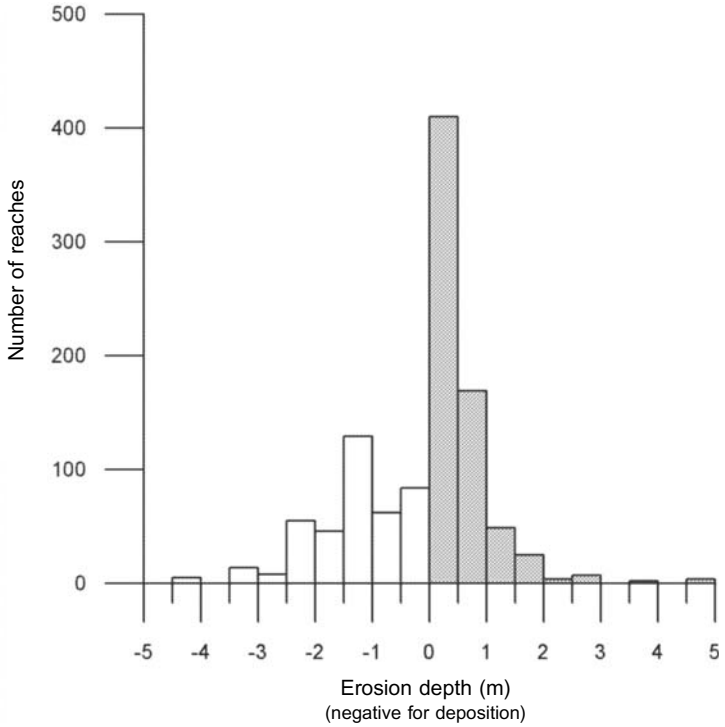

Figure 7.10. Queen Charlotte Islands database: histogram of erosion depths for all 1,073 reaches, both confined and unconfined.

Data courtesy Messrs. T. Rollerson, Golder Associates Ltd and M. Wise, Vancouver.

except for slope, channel width, presence or absence of lateral confinement, path azimuth and passing volume.

The average magnitude of events in the database is only 1,100 m^3, and ranges from 50–30,000 m^3. The total estimated volume of debris eroded in all of the events is 200,000 m^3, while that deposited is 17% greater, indicating a measure of inaccuracy in the field estimates.

Figure 7.10 shows the distribution of erosion depths compiled from the database. Table 7.3 gives average erosion depths for various slope categories. The following observations can be made:

- The erosion depths vary from -3 m (deposition) to 3 m (erosion), with a few exceptional cases reaching the range of -5 to 5 m.
- The erosion depth exhibits a Poisson distribution within the erosional domain, while being rather uniform in the depositional domain.
- The average value is approximately 0.5 m for all eroding reaches and -1.0 for all depositing reaches. However, the standard deviation exceeds the mean at all slopes, indicating significant skewness in the distributions. The range of observed values is always at least ± 2 m (except at angles exceeding 40°).

Table 7.3. Queen Charlotte Islands database: yield rates in relation to channel slope and confinement.
Data courtesy Messrs. T. Rollerson, Golder Associates Ltd. and M. Wise, Vancouver.

	Unconfined		Confined	
Slope angle	Average	Shaded deviation	Average	Standard deviation
All	−0.94	39.50	0.26	11.62
0–15	−22.33	58.66	−10.89	18.99
16–20	1.55	33.13	2.07	5.57
21–30	5.53	30.75	3.41	6.55
31–50	11.10	12.96	3.88	3.23

Scatter plots correlating erosion depth with path width, cumulative volume of debris passing into the reach, slope angle, and other variables, showed very weak trends and extreme scatter. It was concluded that those variables available in the database (i.e., confinement, path width, slope angle, path azimuth, and passing volume) do not have a significant systematic influence on the erosion depth. Any model using these data must therefore treat D_i as a random variable, with a range of at least −3 to 3 m.

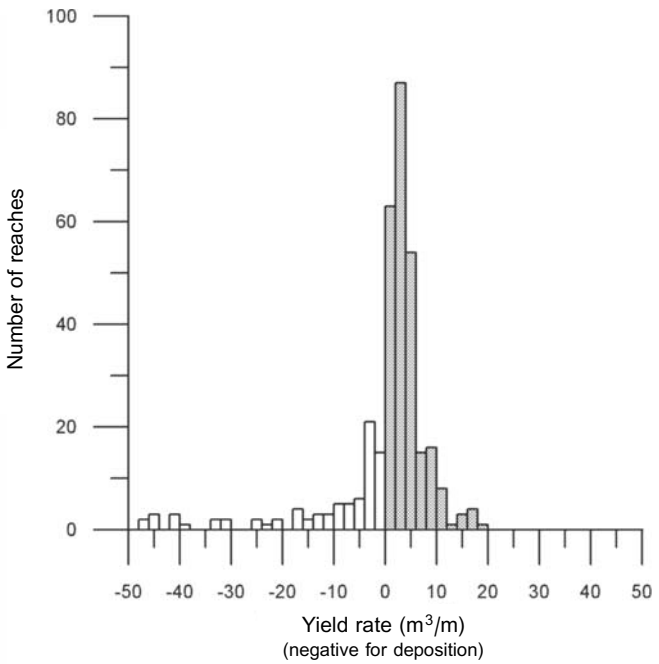

Figure 7.11. Queen Charlotte Islands database: histogram of yield rates for the 340 confined reaches.

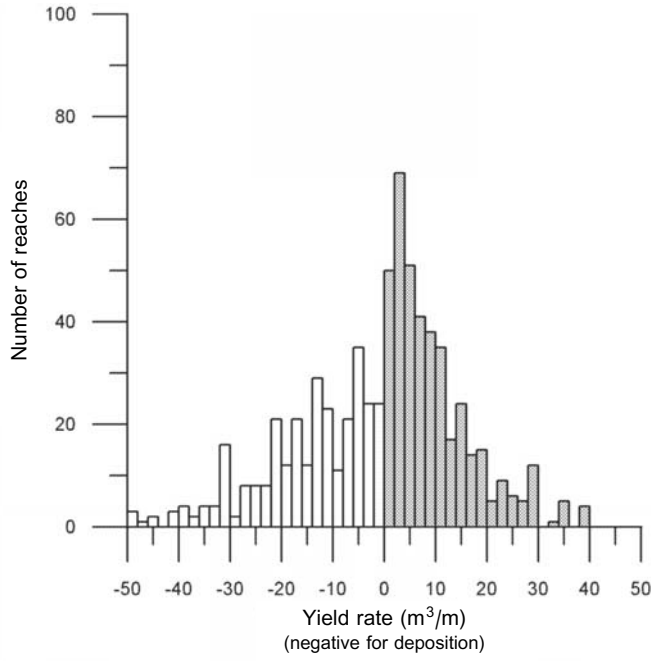

Figure 7.12. Queen Charlotte Islands database: histogram of yield rates for the 733 unconfined reaches.

The distributions of yield rates in all confined and unconfined reaches of the database are shown in Figures 7.11 and 7.12 respectively. In both instances the distributions are approximately normal, centered at a slightly positive value. A summary of means and standard deviations for these data is given in Table 7.4. It is interesting to note that the distributions show a similar trend to the worldwide values compiled in Table 7.2. Thus, the distributions appear to represent typical conditions for relatively small debris flows and debris avalanches.

Figures 7.13 and 7.14 represent an attempt to delineate zones of erosion (full symbols) and deposition (open symbols) in terms of slope angle and the volume of

Table 7.4. Queen Charlotte Islands database: erosion depths (in meters) in relation to channel slope and confinement.

	Unconfined		Confined	
Slope angle	Average	Shaded deviation	Average	Standard deviation
All	0.0	1.2	0.2	1.1
0–15	−1.2	0.9	−0.9	1.4
16–20	−0.1	1.1	0.2	0.8
21–30	0.3	1.0	0.5	0.8
31–50	0.7	0.7	0.6	0.7

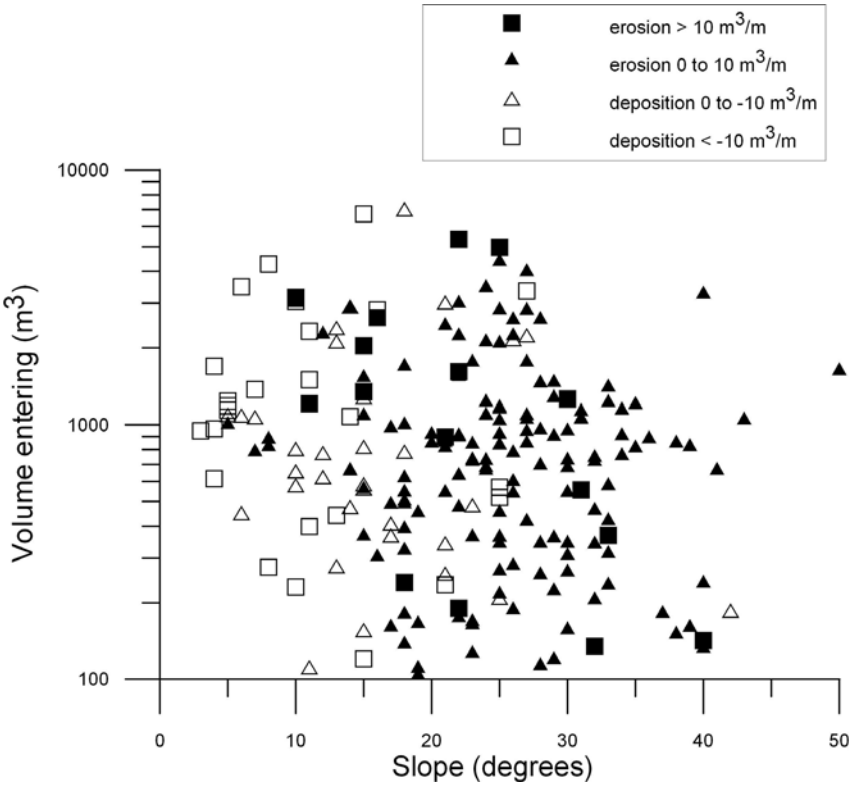

Figure 7.13. Queen Charlotte Islands database: dependence of yield and lag rates on slope angle and the amount of debris flow material entering the reach for "confined" reaches.

debris-flow material entering a given reach. In the case of confined reaches, there appears to be a crude trend, indicating that erosion can occur on slopes as low as 10°, provided that the flow is already fully developed. On the other hand, the volume entering a reach seems to have no effect in unconfined reaches (Figure 7.14). In both cases, there is a transitional zone, at least 10° wide, as well as numerous outliers. Indeed, the occurrence of erosion and deposition in these small magnitude events appears to be a largely random process.

7.8 CONCLUSIONS

The ability to determine entrainment is a crucial step in prediction of debris flow and debris avalanche magnitude and behavior. As shown in this chapter, analytical techniques are unlikely to be useful in the foreseeable future. Empirical relations must be developed, but this task is made complex by the wide scatter in the available data sets, combined with the difficulty of acquiring such data and their generally low level

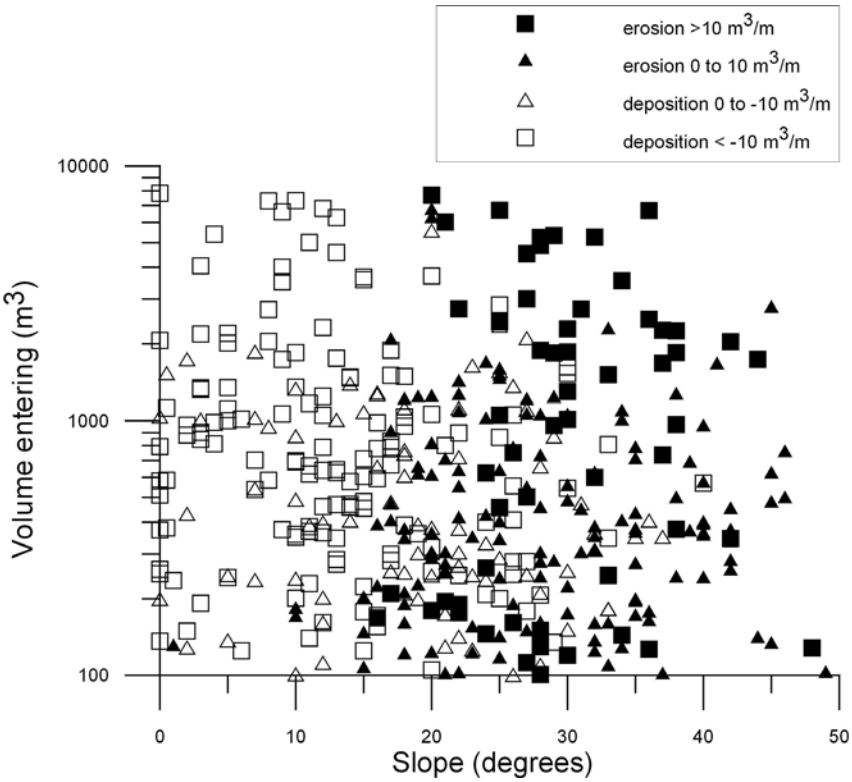

Figure 7.14. Queen Charlotte Islands database: dependence of yield and lag rates on slope angle and the amount of debris flow material entering the reach for "unconfined" reaches.

of reliability. Although difficult, the approach of collecting data on entrainment depth and yield rate, then correlating these data with well-chosen descriptive parameters in a statistical treatment seems to be the only course available. Any such methodology will probably always need to be complemented by judgment.

7.9 REFERENCES

Agostino, V.D. and Marchi, L. (2003) Geomorphological estimation of debris-flow volumes in alpine basins. In: D. Rickenman and L-C. Chen (eds), *Proceedings of the 3rd International Conference on Debris-flow Hazards Mitigation: Mechanics, Prediction and Assessment* (pp. 1097–1106). Millpress, Rotterdam.

Bagnold, R.A. (1966) *An Approach to the Sediment Transport Problem from General Physics: Physiographic and Hydraulic Studies* (USGS Professional Paper 422-I). US Geological Survey, Washington, DC.

Benda, L.E. and Cundy, T.W. (1990) Predicting deposition of debris flows in mountain channels. *Canadian Geotechnical Journal*, **27**, 409–417.

Benda, L. and Dunne, T. (1997) Stochastic forcing of sediment supply to channel networks from landsliding and debris flow. *Water Resources Research*, **33**(12), 2849–2863.

Bovis, M.J. and Dagg, B.R. (1988) A model for debris accumulation and mobilization in steep mountain streams. *Hydrological Sciences Journal*, **33**(6), 589–604.

Bovis, M. and Jakob, M. (1999) The ratio of debris supply in predicting debris flow activity. *Earth Surface Processes and Landforms*, **24**, 1039–1054.

Campbell, D. and Church, M. (2003) Reconnaissance sediment budgets for Lynn Valley, British Columbia: Holocene and contemporary time scales. *Canadian Geotechnical Journal*, **40**, 701–713.

Cannon, S.H. (1993) An empirical model for the volume-change behavior of debris flows. In: H.W. Shen, S.T. Su and F. Wen (eds), *Proceedings of Hydraulic Engineering '93, San Francisco* (Vol. 2, pp. 1768–1773). American Society of Civil Engineers, New York.

Cenderelli, D.A. and Kite, J.S. (1998) Geomorphic effects of large debris flows on channel morphology at North Fork Mountain, eastern West Virginia, USA. *Earth Surface Processes and Landforms*, **23**, 1–19.

Davies, T.R.H. (1986) Large debris flows: A macroviscous phenomena. *Acta Mechanica*, **63**, 161–178.

Easterbrook, D.J. (1999) *Surface Processes and Landforms* (2nd edn, 546 pp.). Prentice Hall, Englewood Cliffs, NJ.

Ellen, S.D., Mark, R.K., Cannon, S.H., and Knifong, D.C. (1993) *Map of Debris Flow Hazards in the Honolulu District of Oahu, Hawaii* (USGS Open File 93-213). US Geological Survey, Reston, VA.

Fannin, R.J. and Rollerson, T.P. (1993) Debris flows: Some physical characteristics and behaviour. *Canadian Geotechnical Journal*, **30**, 71–81.

Fannin, R.J. and Wise, M.P. (2001) An empirical-statistical model for debris flow travel distance. *Canadian Geotechnical Journal*, **38**, 982–994.

Franks, C.A.M. (1999) Characteristics of some rainfall-induced landslides on natural slopes, Lantau Island, Hong Kong. *Quarterly Journal of Engineering Geology*, **32**, 247–259.

Guadagno, F.M., Martino, S., and Scarascia-Magnozza, G. (2003) Influence of man-made cuts on the stability of pyroclastic covers (Campania, southern Italy): A numerical approach. *Environmental Geology*, **43**, 371–384.

Hungr, O. (2000) Analysis of debris flow surges using the theory of uniformly progressive flow. *Earth Surface Processes and Landforms*, **25**, 1–13.

Hungr, O., Morgan, G.C., and Kellerhals, R. (1984) Quantitative analysis of debris torrent hazards for design of remedial measures. *Canadian Geotechnical Journal*, **21**, 663–677.

Hutchinson, J.N. and Bhandari, R.K. (1971) Undrained loading, a fundamental mechanism of mudflows and other mass movements. *Géotechnique*, **21**, 353–358.

Ikeya, H. (1981). A method of designation for area in danger of debris flow. *Erosion and Sediment Transport in Pacific Rim Steeplands* (IAHS Publication No. 132, pp. 576–588). International Association of Hydrological Sciences, Wallingford, UK.

Iverson, R.M. (1997) The physics of debris flows. *Reviews of Geophysics*, **35**(3), 245–296.

Jakob, M., Hungr, O., and Thomson, B. (1997) Two debris flows with anomalously high magnitude. In: C-L. Chen (ed.), *Proceedings of the 1st International Conference on Debris-flow Hazards Mitigation: Mechanics, Prediction and Assessment* (pp. 382–394). American Society of Civil Engineers, New York.

Jakob, M., Anderson, D., Fuller, T., Hungr, O., and Ayotte, D. (2000). An unusually large debris flow at Hummingbird Creek, Mara Lake, British Columbia. *Canadian Geotechnical Journal*, **37**, 1109–1125.

Jakob M., Bovis, M., and Oden, M. (2004a) Estimating debris flow magnitude and frequency from channel recharge rates. *Earth Surface Processes and Landforms*, in print.

Jakob, M., Porter, M., Savigny, K.W., and Yaremko, E. (2004b) A geomorphic approach to the design of pipeline crossings of mountain streams. *Proceedings of IPC 2004 International Pipeline Conference, October 4–8, 2004, Calgary* (in print).

Johnson, A.M. (1970) *Physical Processes in Geology* (577 pp.). W.H. Freeman, New York.

Jordan, M. (1994) Debris flows in the Southern Coast Mountains, British Columbia: Dynamic behaviour and physical properties (250 pp.). Ph.D. Thesis (Geography), University of British Columbia, Vancouver.

King, J. (1996) *Tsing Shan Debris Flow* (Special Project Report SPR 6/96, 133 pp.). Geotechnical Engineering Office, Hong Kong Government.

Lau, K.C. and Woods, N.W. (1997) Review of methods for predicting travel distance of debris from landslides on natural terrain (Geotechnical Engineering Office, Hong Kong, Technical Note, TN 7/97, 48 pp.).

Li, J., Jianmo, Y., Cheng, B., and Defu, L. (1983) The main features of the mudflow in Jiang-Jia Ravine. *Zeitschrift für Geomorphologie*, **27**(3), 325–341.

Li, J. and Yuan, J. (1983) The main features of the mudflow in Jiang-Jia Ravine. *Zeitschrift Geomophologie*, **27**, 325–341.

Lopez, J.L., Perez, D., and Garcia, R. (2003) Hydrologic and geomorphological evaluation of the 1999 debris flow event in Venezuela. *Third International Conference on Debris Flow Hazards Mitigation: Mechanics, Prediction and Assessment* (Davos, Switzerland), **2**, 989–1000

Morgenstern. N.R. and Sangrey (1978) Methods of slope stability analysis. In: R.J. Schuster and R.J. Krizek (eds), *Landslides, Analysis and Control* (Special Report 176, pp. 155–171). Transportation Research Board, National Academy of Sciences, Washington, DC.

Okubo, S. and Mizuyama, T. (1981) Planning of countermeasures against debris flow. *Civil Engineering Journal*, **23**(9) [in Japanese].

Okuda, S., Suwa, H., Okunishi, K., Yokohama, K., and Ogawa, K. (1980) Synthetic observation on debris flow. *Annals of the Disaster Prevention Research Institute, Kyoto University*, **24**, 411–448.

Pierson, T.C. (1995) Flow characteristics of large eruption-triggered debris flows at snow-clad volcanoes: Constraints for debris-flow models. *Journal of Volcanology and Geothermal Research*, **66**, 283–294.

Revellino, P., Hungr, O., Guadagno, F.M., and Evans, S.G. (2003) Velocity and runout prediction of destructive debris flows and debris avalanches in pyroclastic deposits, Campania Region, Italy. *Environmental Geology*, **45**, 295–311.

Rickenmann, D., Weber, D., and Stepanov, B. (2003) Erosion by debris flows in field and laboratory experiments. In: D. Rickenman and L-C. Chen (eds), *Proceedings of the 3rd International Conference on Debris-flow Hazards Mitigation: Mechanics, Prediction and Assessment* (pp. 883–893). Millpress, Rotterdam.

Sassa, K. (1985). The mechanism of debris flows. In: *Proceedings of the XI International Conference on Soil Mechanics and Foundation Engineering, San Francisco* (Vol. 1, pp. 1173–1176).

Springer, G.S., Dowdy, H.S., and Eaton, L.S. (2001) Sediment budgets for two mountainous basins affected by a catastrophic storm: Blue Ridge Mountains, Virginia. *Geomorphology*, **37**, 135–148.

Takahashi, T. (1978) Mechanical characteristics of debris flow. *Journal of the Hydraulics Division, ASCE*, **104**(HY8), 1153–1169.

Takahashi, T. (1991). *Debris Flow* (IAHR Monograph, 165 pp.). A.A. Balkema, Rotterdam.

Thurber Consultants Ltd (1983) *Debris Torrent and Flooding Hazards, Highway 99, Howe Sound* (Report, 42 pp.). British Columbia Ministry of Transportation and Highways, Victoria, Canada.VanDine, D.F. (1985) Debris flows and debris torrents in the Southern Canadian Cordillera. *Canadian Geotechnical Journal*, **22**, 44–68.

Wise, M.P. (1997) Probabilistic modelling of debris flow travel distance using empirical volumetric relationships. Master of Applied Science thesis, University of British Columbia, Vancouver.

Wong, H.N., Ho, K.K.S., and Chan, Y.C. (1997) Assessment of consequence of landslides. In: R. Fell and D.M. Cruden (eds), *Proceedings of the Landslide Risk Workshop* (pp. 111–126). A.A. Balkema, Rotterdam.